

Notch–RBP-J signaling regulates the transcription factor IRF8 to promote inflammatory macrophage polarization

Haixia Xu^{1,2,9}, Jimmy Zhu^{1,9}, Sinead Smith^{1,9}, Julia Foldi³, Baohong Zhao¹, Allen Y Chung¹, Hasina Outtz⁴, Jan Kitajewski⁴, Chao Shi^{3,5}, Silvio Weber⁶, Paul Saftig⁶, Yueming Li⁵, Keiko Ozato⁷, Carl P Blobel¹, Lionel B Ivashkiv^{1,3} & Xiaoyu Hu^{1,8}

Emerging concepts suggest that the functional phenotype of macrophages is regulated by transcription factors that define alternative activation states. We found that RBP-J, the main nuclear transducer of signaling via Notch receptors, augmented Toll-like receptor 4 (TLR4)-induced expression of key mediators of classically activated M1 macrophages and thus of innate immune responses to *Listeria monocytogenes*. Notch–RBP-J signaling controlled expression of the transcription factor IRF8 that induced downstream M1 macrophage-associated genes. RBP-J promoted the synthesis of IRF8 protein by selectively augmenting kinase IRAK2-dependent signaling via TLR4 to the kinase MNK1 and downstream translation-initiation control through eIF4E. Our results define a signaling network in which signaling via Notch–RBP-J and TLRs is integrated at the level of synthesis of IRF8 protein and identify a mechanism by which heterologous signaling pathways can regulate the TLR-induced inflammatory polarization of macrophages.

Macrophages serve essential sentinel and effector functions in innate immunity and the transition to adaptive immunity. Depending on the environmental cues present, macrophages can assume a spectrum of activation states ranging from classically activated M1 inflammatory macrophages to various alternatively activated M2 macrophages that are involved in immunoregulation and tissue repair¹. M1 macrophages are characterized by the production of inflammatory mediators, such as interleukin 12 (IL-12) and inducible nitric oxide synthase (iNOS), in response to microbial product-mediated activation of Toll-like receptors (TLRs) and cytokines such as interferon- γ (IFN- γ)¹. In contrast, M2 macrophages have lower expression of inflammatory mediators and have key roles in wound healing, host defense against helminths and the resolution of inflammation¹. Published work has linked specific transcription factors to functional phenotypes of macrophage^{2,3}, which suggests a parallel to T cell biology, in which lineage-specific transcription factors regulate cell differentiation. Members of the interferon-regulatory factor (IRF) family of proteins are transcriptional regulators of macrophage polarization, with IRF5 and IRF4 associated with polarization to the M1 state and M2 state, respectively^{2,3}. IRF8 is induced by IFN- γ and contributes to the induction of several genes, including *Ifnb1* (which encodes IFN- β)⁴, *I12b* (which encodes the p40 subunit of IL-12 (IL-12p40))⁵, *I12a* (which encodes the p35 subunit of IL-12)⁶ and *Nos2* (which encodes iNOS)⁷, in response to stimulation via TLRs and thus has a

role in host defense against intracellular pathogens such as vaccinia virus and *Leishmania major*⁸. In the immune system, IRF8 also regulates the development of the lymphoid and myeloid lineages and is indispensable for generation of plasmacytoid dendritic cell and CD8⁺ dendritic cell populations^{9,10}.

The stimulation of TLRs activates at least three main downstream signaling pathways, the transcription factor NF- κ B pathway, the mitogen-activated protein kinase (MAPK) pathway and the IRF pathway¹¹, to induce gene transcription. However, TLR responses are also modulated by a variety of post-transcriptional mechanisms, including regulation of the decay and transport of mRNA and the control of translation initiation¹². Translation-control mechanisms often target the process of translation initiation, during which the recruitment and assembly of translation-initiation factors, including the main cap-binding protein eIF4E, on target mRNA activates translation¹³. Cytokines, chemokines and enzymes are often targets of translational control¹². Whether translational regulation controls other molecules, such as signaling intermediates and transcription factors, remains an open question.

The Notch signaling pathway regulates the differentiation, proliferation, survival and development of cells¹⁴. Ligation of Notch receptors by their ligands leads to cleavage of Notch by proteases of the ADAM family and subsequent intramembranous cleavage by a γ -secretase to release the Notch intracellular domain (NICD).

¹Arthritis and Tissue Degeneration Program, Hospital for Special Surgery, New York, New York, USA. ²Department of Endocrinology, the third Affiliated Hospital of Sun Yat-Sen University, Guangzhou, China. ³Graduate Program in Immunology and Microbial Pathogenesis, Weill Cornell Graduate School of Medical Sciences, New York, New York, USA. ⁴Herbert Irving Comprehensive Cancer Center, Columbia University, New York, New York, USA. ⁵Memorial Sloan Kettering Cancer Center, New York, New York, USA. ⁶Biochemisches Institute, Christian Albrechts Universität Kiel, Kiel, Germany. ⁷National Institute of Child Health and Human Development, National Institutes of Health, Bethesda, Maryland, USA. ⁸Department of Medicine, Weill Cornell Medical College, New York, New York, USA. ⁹These authors contributed equally to this work. Correspondence should be addressed to X.H. (hux@hss.edu).

Received 30 January; accepted 5 April; published online 20 May 2012; doi:10.1038/ni.2304

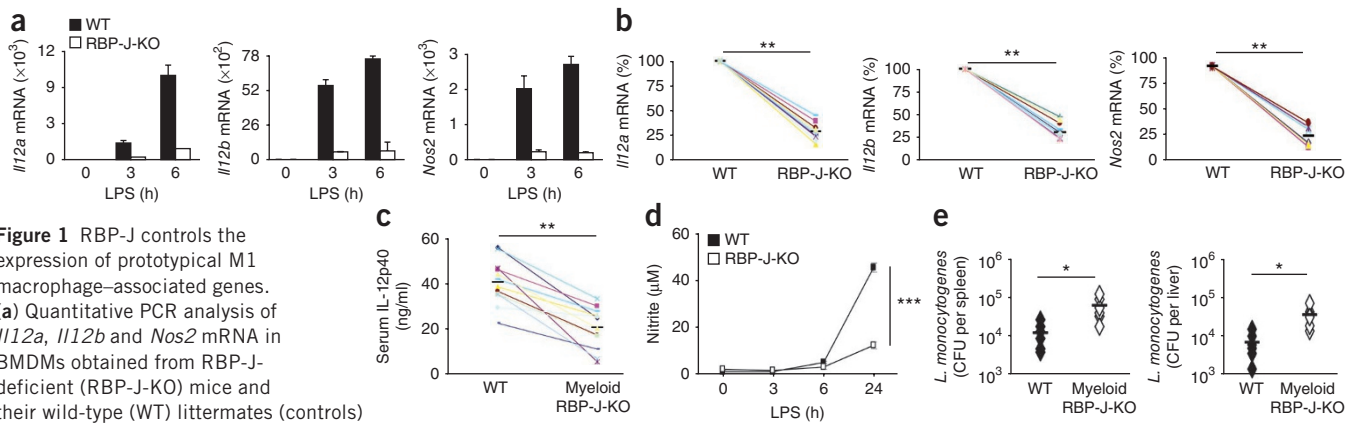


Figure 1 RBP-J controls the expression of prototypical M1 macrophage-associated genes. **(a)** Quantitative PCR analysis of *Il12a*, *Il12b* and *Nos2* mRNA in BMDMs obtained from RBP-J-deficient (RBP-J-KO) mice and their wild-type (WT) littermates (controls) and stimulated for 0–6 h (horizontal axes) with LPS (1 ng/ml); results are normalized to *Gapdh* mRNA (encoding glyceraldehyde phosphate dehydrogenase) and are presented relative to those of unstimulated wild-type cells, set as 1. **(b)** Quantitative PCR analysis of mRNA from wild-type and RBP-J-deficient BMDMs stimulated for 3 or 6 h with LPS (all colors indicate 3 h, except yellow and magenta (6 h)); results are presented relative to maximal mRNA expression in wild-type cells, set as 100%. **(c)** Enzyme-linked immunosorbent assay of IL-12p40 in the serum of mice with myeloid-specific deletion of RBP-J (Myeloid RBP-J-KO) and wild-type mice ($n = 12$ per group) given intraperitoneal injection of 200 μ g LPS, followed by collection of blood 3 h later. **(d)** Release of nitric oxide into supernatants of wild-type and RBP-J-deficient BMDMs treated with LPS, measured as the nitric oxide metabolite nitrite. **(e)** Bacterial loads in the spleens and livers of chimeras reconstituted with bone marrow with myeloid-specific deletion of RBP-J or wild-type bone marrow, then infected intravenously with 3×10^3 *L. monocytogenes* strain 10403S, analyzed day 3.5 later as colony-forming units (CFU). Each symbol (**b,c,e**) represents an individual mouse; small horizontal lines indicate the average (**b,c**) or mean (**e**). * $P < 0.05$, ** $P < 0.001$ and *** $P < 0.0001$ (Student's *t* test). Data are representative of six experiments (**a**; mean and s.d. of triplicates), three independent experiments (**d**; mean and s.d. of triplicates) or one experiment (**e**; $n = 6$ mice per group) or are pooled from six to twelve independent experiments (**b,c**).

The NICD translocates to the nucleus and binds to the DNA-binding protein RBP-J (also called CSL or CBF1)¹⁴. In the immune system, the most established functions for Notch signaling are in regulating the development and function of lymphocytes¹⁵. Published data also suggest a role for the Notch pathway in regulating the differentiation and function of myeloid cells^{16–24}. However, the mechanism of action of the Notch–RBP-J pathway in macrophage polarization is unknown.

In this study we found that the Notch–RBP-J pathway controlled the expression of prototypical M1 effector molecules such as IL-12 and iNOS, and promoted host defense against the intracellular pathogen *Listeria monocytogenes*. We identified IRF8 as a downstream target of the Notch–RBP-J pathway and found that RBP-J regulated the translation of IRF8 by selectively modulating TLR4 signaling through activation of the kinase MNK1 mediated by the upstream signaling molecule IRAK2 and the initiation of translation controlled by eIF4E. Our studies delineate a signaling network in which the Notch–RBP-J and TLR signaling pathways are integrated at the level of synthesis of IRF8 protein to regulate induction of the M1 phenotype in macrophages.

RESULTS

RBP-J controls M1 macrophage-associated genes

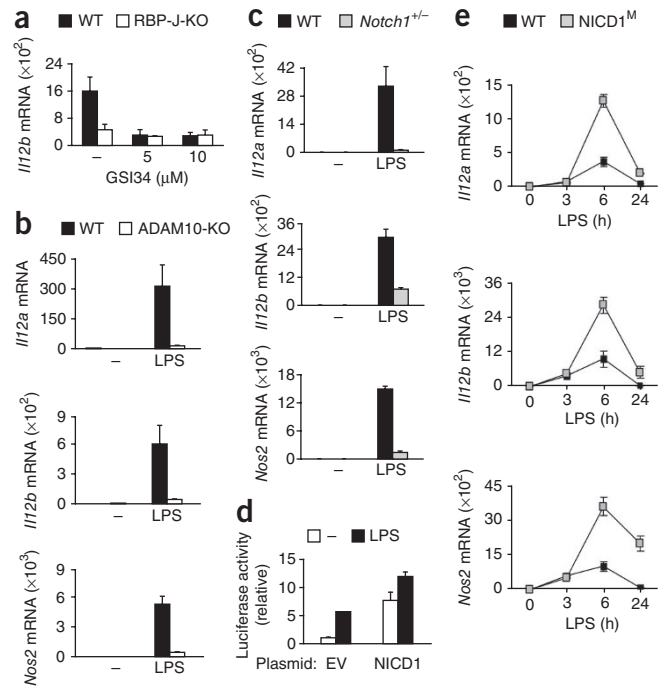
To investigate the role of the Notch–RBP-J pathway in macrophage activation, we profiled the gene expression of wild-type and RBP-J-deficient bone marrow-derived macrophages (BMDMs) stimulated with the TLR4 ligand lipopolysaccharide (LPS), which induces the expression of key M1 macrophage-associated proteins, such as IL-12 and iNOS¹. We confirmed efficient deletion of RBP-J in BMDMs from RBP-J-deficient mice (with loxP-flanked *Rbpj* alleles deleted by Cre recombinase expressed under control of the interferon-inducible gene *Mx1*; *Rbpj*^{fllox/fllox}*Mx1*-Cre mice) by assessing the expression of *Rbpj* mRNA and RBP-J protein (**Supplementary Fig. 1a,b**). Microarray analysis showed that approximately 10% of TLR4-inducible genes were partially dependent on RBP-J and that a very broad range of TLR target genes were induced to a normal amount in RBP-J-deficient

macrophages and thus were RBP-J independent (**Supplementary Fig. 1c** and data not shown). However, a small number of LPS-induced genes (fewer than ten) were essentially completely dependent on RBP-J (expression >80% lower in RBP-J-deficient cells; data not shown). Among those genes, we confirmed by quantitative PCR the dependence of *Il12a*, *Il12b* and *Nos2* on RBP-J expression (**Fig. 1a,b**).

To assess the functional and physiological relevance of RBP-J-mediated regulation of M1 macrophage-associated genes, we examined the *in vivo* expression of IL-12 protein in the myeloid compartment under conditions of inflammation. After endotoxin challenge, mice with myeloid-specific deletion of RBP-J (with loxP-flanked *Rbpj* alleles deleted by Cre recombinase expressed under control of the myeloid cell-specific gene *Lyz2*; *Rbpj*^{fllox/fllox}*Lyz2*-Cre mice) had significantly lower serum concentrations of IL-12p40 protein than did their wild-type littermates (control mice; **Fig. 1c**). The production of nitric oxide in macrophages is catalyzed by iNOS. In response to stimulation with LPS, RBP-J-deficient macrophages produced significantly less nitric oxide than did wild-type cells, as assessed by the concentration of the nitric-oxide metabolite nitrite (**Fig. 1d**). Because IL-12 and iNOS mediate responses to intracellular bacteria, we assessed the role of RBP-J *in vivo* in host defense against *L. monocytogenes*, an intracellular pathogen whose successful clearance requires effectors of M1 macrophages, such as IL-12 and iNOS²⁵. Chimeric mice generated with bone marrow cells from mice with RBP-J deficiency in the myeloid lineage (*Rbpj*^{fllox/fllox}*Lyz2*-Cre mice) were more susceptible to *L. monocytogenes* infection than were chimeras generated with bone marrow cells from control (*Rbpj*^{+/+}*Lyz2*-Cre) mice, as demonstrated by the significantly greater bacterial burden in the spleens and livers of infected mutant mice (**Fig. 1e**). Together these results showed that RBP-J was essential for the expression of genes characteristic of the core M1 macrophage response *in vitro* and for the manifestation of key myeloid effector functions *in vivo*.

In addition to promoting the expression of M1 macrophage-associated genes, RBP-J suppressed the expression of a group of genes characteristic of the M2 macrophage phenotype, a result obtained

Figure 2 Induction of RBP-J-dependent M1 macrophage-associated genes requires canonical Notch signaling. (a) Quantitative PCR analysis of *Il12b* mRNA in BMDMs obtained from paired wild-type and RBP-J-deficient littermates and given no pretreatment (–) or pretreated for 48 h with the γ -secretase inhibitor GSI34 and then stimulated for 3 h with LPS (1 ng/ml); results are normalized to *Gapdh* mRNA and are presented relative to those of unstimulated wild-type cells, set as 1. (b,c) Quantitative PCR analysis of *Il12a*, *Il12b* and *Nos2* mRNA in wild-type and ADAM10-deficient (ADAM10-KO) BMDMs (b) or BMDMs obtained from *Notch1*^{+/-} mice and their wild-type littermates (c), left unstimulated (–) or stimulated for 3 h with LPS; results presented as in a. (d) Luciferase activity in lysates of RAW264.7 mouse macrophages transfected with an *Il12b* luciferase reporter construct plus empty vector (EV) or an expression plasmid for NICD1, followed by no stimulation (–) or stimulation for 6 h with LPS (1 μ g/ml) at 36 h after transfection; results are normalized to values for renilla luciferase and are presented relative to those of unstimulated cells transfected with empty vector, set as 1. (e) Quantitative PCR analysis of *Il12a*, *Il12b* and *Nos2* mRNA in BMDMs obtained from NICD1^M mice and their wild-type littermate and stimulated for 0–24 h (horizontal axes) with LPS; results presented as in a. Data are representative of at least three independent experiments (mean and s.d. of triplicates).



by microarray analysis that we confirmed by quantitative PCR (Supplementary Fig. 1d). RBP-J suppressed the expression of JMJD3, the key inducer of M2 polarization³, which indicated that RBP-J had an inhibitory role in the M2 differentiation program. Although these results suggested that RBP-J might regulate the balance between M1 polarization and M2 polarization, in this study we focused on delineating the mechanisms by which RBP-J regulates the M1 program.

RBP-J controls M1 macrophage genes downstream of Notch

RBP-J has a key role in signal transduction via the canonical Notch pathway. However, Notch-independent RBP-J activities have been reported¹⁴. To assess the role of the canonical Notch pathway in the RBP-J-mediated regulation of M1 macrophage-associated genes, we used GSI34, a chemical inhibitor of γ -secretase, to abolish signaling from the Notch receptors. The treatment of wild-type mouse BMDMs with GSI34 did not have any detectable toxic effects (data not shown), yet it effectively suppressed the LPS-induced expression of *Il12b* (Fig. 2a), which suggested that the induction of *Il12b* by LPS required canonical Notch signaling. The inhibition of γ -secretase by GSI34 had no effect on the already blunted *Il12b* expression in RBP-J-deficient macrophages (Fig. 2a), which indicated that γ -secretase and RBP-J function in a linear pathway. Another proteolytic event required for the activation of Notch signaling is the cleavage of receptors by proteases of the ADAM family, mainly ADAM10 (ref. 14). Deficiency in ADAM10 almost completely abolished induction of the RBP-J-dependent genes *Il12a*, *Il12b* and *Nos2* by LPS in macrophages (Fig. 2b). In contrast, deficiency in ADAM17 did not notably alter the LPS-induced expression of RBP-J-dependent M1 macrophage-associated genes such as *Il12b* (Supplementary Fig. 2a and data not shown).

We next sought to determine which Notch receptors were responsible for the activation of the M1 macrophage-associated genes. Resting mouse BMDMs expressed mainly Notch1 and Notch2 (data not shown). To assess the role of Notch1 in the expression of M1-macrophage-associated genes, we used macrophages from mice heterozygous for the deletion of *Notch1* (*Notch1*^{+/-} mice), as complete deletion of *Notch1* leads to death²⁶. *Notch1* haploinsufficiency was characterized by approximately 70–80% lower expression of *Notch1* mRNA (Supplementary Fig. 2b)²⁴. *Notch1*^{+/-} macrophages showed profound defects in the induction of RBP-J-dependent M1 macrophage-associated genes (Fig. 2c), which mimicked the effects

of RBP-J deletion (Fig. 1a,b), inhibition with γ -secretase (Fig. 2a) and ADAM10 deficiency (Fig. 2b). In contrast to deletion of Notch1, knocking down the expression of Notch2 did not alter the LPS-mediated induction of RBP-J-dependent genes such as *Il12b* (Supplementary Fig. 2c). Knockdown of Notch2 expression in *Notch1*^{+/-} cells did not further diminish *Il12b* expression (Supplementary Fig. 2c), which suggested that Notch2, either alone or in concert with Notch1, did not contribute much to the induction of RBP-J-dependent M1 macrophage-associated genes. Next we assessed Notch1 function by gain-of-function approaches. Forced expression of the NICD of Notch1 (NICD1) activated a reporter construct driven by the mouse *Il12b* promoter (Fig. 2d). We also generated mice with constitutive expression of NICD1 in myeloid cells (called 'NICD1^M mice' here) by crossing *Lyz2-Cre* mice with mice expressing NICD1 from the ubiquitous *Rosa26* locus²⁷. BMDMs from NICD1^M mice were morphologically undistinguishable from wild-type macrophages and expressed markers of mature macrophages (Supplementary Fig. 3a–c). NICD1^M BMDMs had higher NICD1 expression and constitutively active Notch signaling than did wild-type cells, as assessed by expression of the canonical Notch target gene *Hes1* (Supplementary Fig. 3d and data not shown). Stimulation with LPS resulted in greater induction of M1 macrophage-associated genes in NICD1^M macrophages than in control macrophages (Fig. 2e). Collectively, these results indicated that the Notch1–ADAM10– γ -secretase–RBP-J axis regulated the expression of M1 macrophage-associated genes.

RBP-J controls IRF8 expression and function

Il12a, *Il12b* and *Nos2* are known to share common mechanisms of regulation, such as dependence on the NF- κ B subunit c-Rel^{28–30} and dependence on IRF1 and IRF8 (refs. 6,7,31). In addition, they were all categorized as secondary-response genes³² (Supplementary Fig. 4). We investigated regulation of the expression of c-Rel, IRF1 or IRF8 by the Notch–RBP-J pathway. The expression of c-Rel and IRF1 was not substantially altered by RBP-J deficiency (data not shown), which suggested that they were not targets of RBP-J-mediated regulation. It has been reported that IRF8 expression is regulated at the transcriptional

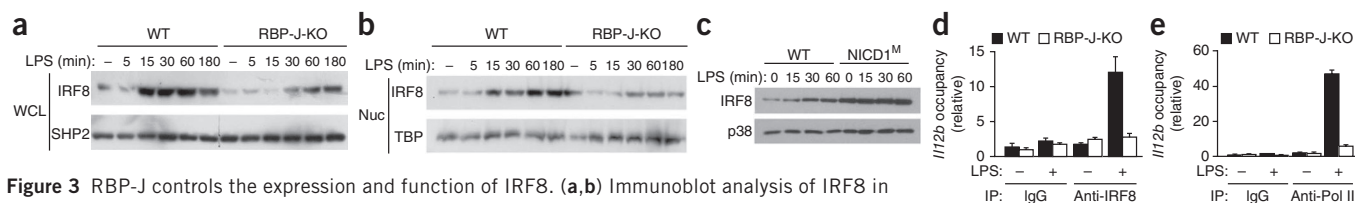


Figure 3 RBP-J controls the expression and function of IRF8. (a,b) Immunoblot analysis of IRF8 in whole-cell lysates (WCL; a) and nuclear extracts (Nuc; b) of BMDMs obtained from paired wild-type and RBP-J-deficient littermates and stimulated for 0–180 min (above lanes) with LPS; SHP2 (a) and TBP (b) serve as loading controls. (c) Immunoblot analysis of IRF8 in whole-cell lysates of BMDMs obtained from NICD1^M mice and their wild-type littermates and stimulated for 0–60 min (above lanes) with LPS; p38 serves as a loading control. (d,e) Chromatin immunoprecipitation (IP) of LPS-treated wild-type and RBP-J-deficient macrophages with the control antibody immunoglobulin G (IgG) or with antibody to IRF8 (Anti-IRF8; d) or antibody to RNA polymerase II (Anti-Pol II; e), followed by quantitative PCR analysis of the promoter region of *I12b* to assess occupancy; results are normalized to those of 28S rRNA and are presented relative to those of unstimulated wild-type cells, set as 1. Data are representative of six (a,b) two (c) or three (d,e) independent experiments (mean and s.d. of triplicates in d,e).

level and that the induction of IRF8 protein follows the induction of *Irf8* mRNA and occurs over the course of hours^{33,34}. In contrast to those published observations, LPS treatment rapidly (within 15 min) and robustly induced the expression of IRF8 protein, as assessed in whole-cell lysates and nuclear extracts of wild-type BMDMs (Fig. 3a,b). We verified the specificity of the detection of IRF8 by immunoblot analysis of IRF8-deficient macrophages (Supplementary Fig. 5a). We confirmed the rapid induction of IRF8 protein in various culture conditions and with several protein-extraction methods (data not shown). In contrast to the robust LPS-dependent induction of IRF8 in wild-type cells, we observed less IRF8 in whole-cell lysates and nuclear extracts of RBP-J-deficient macrophages (Fig. 3a,b). The expression of other members of the IRF family, such as IRF4 and IRF5, was not affected by RBP-J deficiency (Supplementary Fig. 5b). In a gain-of-function approach, IRF8 protein expression was much higher in NICD1^M macrophages than in wild-type macrophages (Fig. 3c). These results suggested that Notch–RBP-J was required for the rapid induction of IRF8 protein after the stimulation of TLR4.

The recruitment of IRF8 to its target-gene promoters is necessary for the binding of RNA polymerase II and subsequent transcriptional activation⁴. Chromatin-immunoprecipitation assays showed that the activation of wild-type macrophages with LPS led to the recruitment of IRF8 to the proximal promoter of *I12b* (Fig. 3d). This effect was almost completely abolished in RBP-J-deficient macrophages (Fig. 3d). There was concomitantly less recruitment of RNA polymerase II to the *I12b* promoter in RBP-J-deficient cells (Fig. 3e), which suggested that the lower abundance of IRF8 in the absence of RBP-J was not sufficient to assemble the transcriptional machinery at the *I12b* promoter. Overall, our data suggested that RBP-J regulated the expression and transcriptional function of IRF8 downstream of TLR signaling.

We next sought to determine whether the lower IRF8 expression in RBP-J-deficient macrophages explained the low expression of M1 macrophage-associated genes in these cells. The induction of *I12a*, *I12b* and *Nos2* by LPS was much lower in IRF8-deficient macrophages than in wild-type cells (Fig. 4a). We determined whether the restoration of IRF8 expression in RBP-J-deficient cells would restore the expression of *I12a*, *I12b* and *Nos2*. Through the use of retroviral transduction, we restored IRF8 expression in RBP-J-deficient macrophages to approximately its expression in wild-type cells (Fig. 4b). Reconstitution with IRF8 nearly completely corrected the defective expression of *I12b* mRNA (Fig. 4c) and IL-12p40 protein (Fig. 4d) in RBP-J-deficient cells. Reconstitution with IRF8 also partially restored the expression of *I12a* in RBP-J-deficient macrophages (Fig. 4c), whereas the impaired *Nos2* expression of RBP-J-deficient cells was not ‘rescued’ by IRF8 reconstitution (Supplementary Fig. 5c), which suggested the involvement of additional factors in RBP-J-regulated

Nos2 expression. These results indicated that RBP-J regulated the expression of M1 macrophage-associated genes at least in part through IRF8.

RBP-J is required for the rapid synthesis of IRF8 protein

Next we investigated the mechanisms by which RBP-J regulates the expression of IRF8 protein. Because IRF8 expression is known to be regulated at the level of mRNA by stimuli such as IFN- γ (refs. 34,35), we investigated whether TLR4 and RBP-J induced the accumulation of *Irf8* mRNA. Stimulation with LPS for up to 3 h did not result in notable upregulation of *Irf8* mRNA at any of the time points assessed (0–180 min, which corresponded to the observed induction of IRF8 protein) in wild-type BMDMs (Fig. 5a). As a control, we observed considerable induction of mRNA encoding tumor-necrosis factor

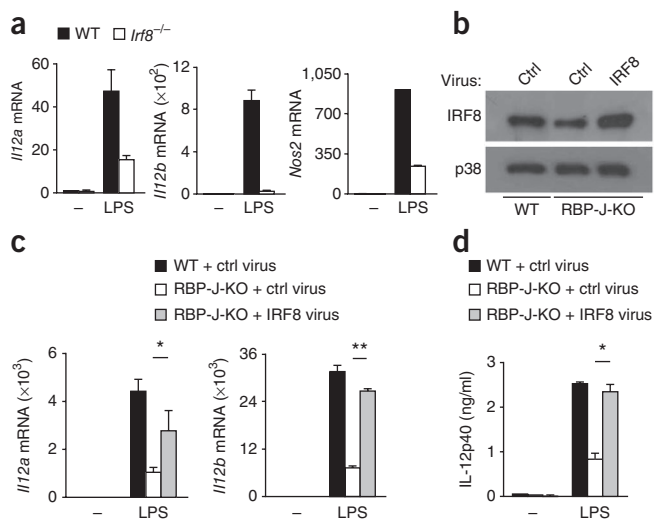
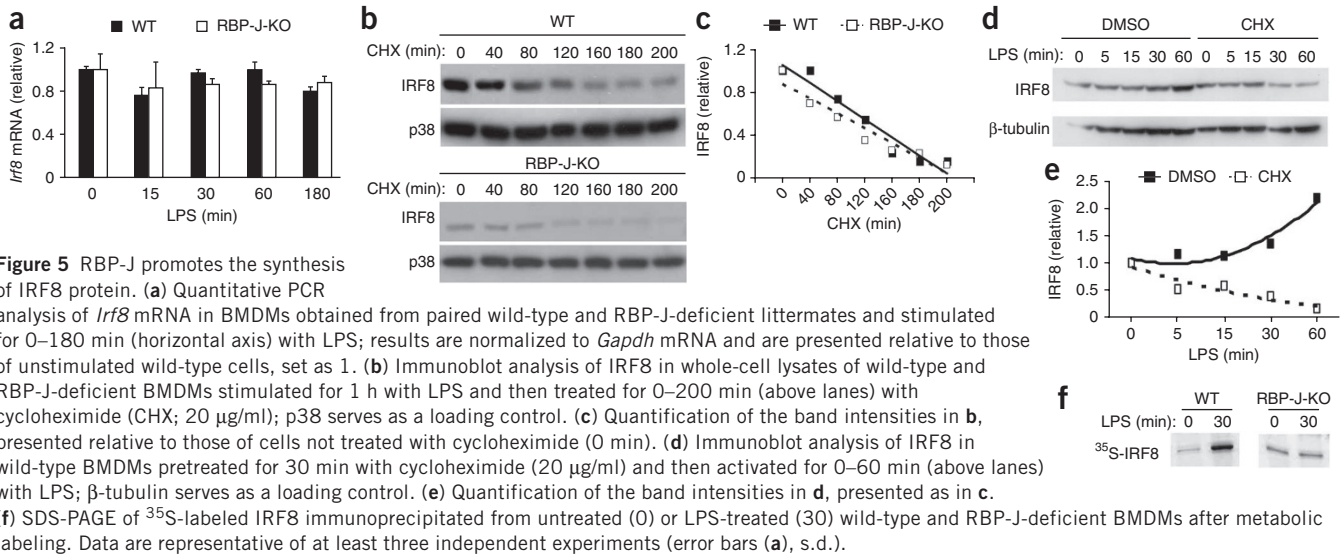


Figure 4 IRF8 mediates RBP-J-dependent activation of the expression of M1 macrophage-associated genes. (a) Quantitative PCR analysis of *I12a*, *I12b* and *Nos2* mRNA in wild-type and *Irf8*^{-/-} BMDMs left unstimulated or stimulated for 3 h with LPS; results are normalized to *Gapdh* mRNA and are presented relative to those of unstimulated wild-type cells, set as 1. (b) Immunoblot analysis of IRF8 in BMDMs obtained from paired wild-type and RBP-J-deficient littermates and transduced with control virus (Ctrl) or retrovirus expressing IRF8; p38 serves as a loading control. (c,d) Quantitative PCR analysis of *I12a* and *I12b* mRNA (c) and enzyme-linked immunosorbent assay of IL-12p40 (d) in the BMDMs in b, stimulated for 6 h with LPS at 48 h after transduction; mRNA results (c) presented as in a. * $P < 0.05$ and ** $P < 0.001$ (Student's *t* test). Data are representative of three (a–c) or two (d) independent experiments (mean and s.d. of triplicates in a,c,d).



after treatment with LPS (**Supplementary Fig. 5d**), and pretreatment with IFN- γ before stimulation with LPS resulted in the induction of *Irf8* mRNA in wild-type macrophages, as expected (**Supplementary Fig. 5e**). We also confirmed the results presented above through the use of distinct quantitative PCR primers that target a region of *Irf8* mRNA³³ upstream of that amplified in **Figure 5a** (data not shown). These results suggested that the rapid induction of IRF8 protein by TLR4 stimulation was not due to higher expression of *Irf8* mRNA. In addition, RBP-J deficiency did not substantially alter the amount of *Irf8* mRNA at baseline or after treatment with LPS (**Fig. 5a**), which suggested that the rapid induction of IRF8 by TLR4 stimulation was regulated at the level of the protein.

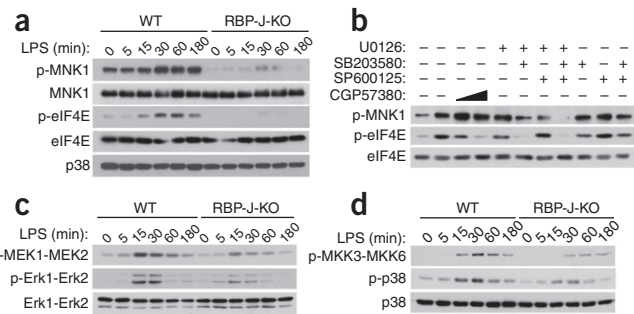
IRF8 is a labile protein³⁶, so we determined whether RBP-J regulated the degradation of IRF8 protein. We added the protein-synthesis inhibitor cycloheximide to LPS-stimulated wild-type or RBP-J-deficient macrophages and monitored the degradation of IRF8 protein over time. Despite the expected difference between wild-type and RBP-J-deficient cells in the abundance of IRF8 protein before treatment with cycloheximide, after cycloheximide treatment, IRF8 protein decreased in a time-dependent manner but independently of RBP-J genotype (**Fig. 5b** and **Supplementary Fig. 5f**). Quantification of IRF8 protein by densitometry showed that in the absence of new protein synthesis, IRF8 protein decayed at a similar rate in wild-type and RBP-J-deficient cells and that its half-life was approximately 150 min in both cell types (**Fig. 5c**), a measurement consistent with the estimate of a published report³⁶. These results suggested that RBP-J did not regulate the degradation of IRF8 protein. However, the addition of cycloheximide to wild-type macrophages before stimulation with LPS blocked the LPS-induced upregulation of IRF8 protein (**Fig. 5d,e**), which suggested that the induction of IRF8 by LPS was the result of new protein synthesis. Metabolic labeling assays showed that stimulation with LPS upregulated the incorporation of 35 S-labeled methionine-cysteine into newly synthesized IRF8 protein in wild-type macrophages but not in RBP-J-deficient cells (**Fig. 5f**). These results suggested that the rapid synthesis of IRF8 protein induced downstream of TLR4 signaling was dependent on RBP-J.

RBP-J controls activation of the MNK1-eIF4E axis

Stimulation via TLRs induces the phosphorylation and activation of kinases of the MNK family and subsequent MNK-mediated

phosphorylation of eIF4E^{37,38}, which is required for the efficient translation of select protein-encoding transcripts³⁹. To investigate the mechanisms by which RBP-J regulates the synthesis of IRF8 protein, we assessed the regulation of MNK1-eIF4E activity by TLR4 and RBP-J. MNK1-eIF4E activity is enhanced by phosphorylation of MNK1 on Thr197 and Thr202, and phosphorylation of eIF4E on Ser209 (ref. 13). TLR4-induced phosphorylation of MNK1 and eIF4E was much lower in RBP-J-deficient macrophages than in wild-type macrophages (**Fig. 6a**). This was not due to lower expression of MNK1 or eIF4E protein (**Fig. 6a**), which suggested that the activation of MNK1-eIF4E downstream of TLR4 signaling required RBP-J.

Activation of MNK1 with subsequent phosphorylation of eIF4E and regulation of translation has been shown to be dependent on the MAPK Erk and stress-activated MAPKs in various systems^{37–39}.



phosphorylation of eIF4E^{37,38}, which is required for the efficient translation of select protein-encoding transcripts³⁹. To investigate the mechanisms by which RBP-J regulates the synthesis of IRF8 protein, we assessed the regulation of MNK1-eIF4E activity by TLR4 and RBP-J. MNK1-eIF4E activity is enhanced by phosphorylation of MNK1 on Thr197 and Thr202, and phosphorylation of eIF4E on Ser209 (ref. 13). TLR4-induced phosphorylation of MNK1 and eIF4E was much lower in RBP-J-deficient macrophages than in wild-type macrophages (**Fig. 6a**). This was not due to lower expression of MNK1 or eIF4E protein (**Fig. 6a**), which suggested that the activation of MNK1-eIF4E downstream of TLR4 signaling required RBP-J.

Activation of MNK1 with subsequent phosphorylation of eIF4E and regulation of translation has been shown to be dependent on the MAPK Erk and stress-activated MAPKs in various systems^{37–39}.

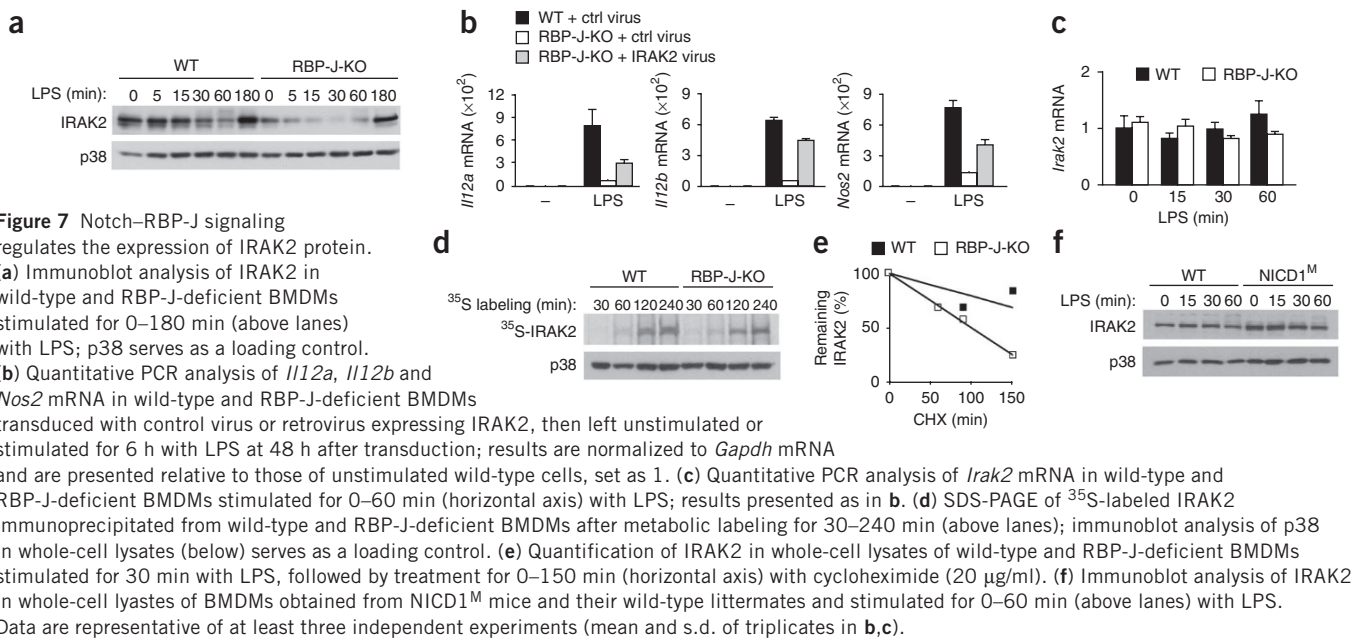


Figure 7 Notch–RBP-J signaling regulates the expression of IRAK2 protein. (a) Immunoblot analysis of IRAK2 in wild-type and RBP-J-deficient BMDMs stimulated for 0–180 min (above lanes) with LPS; p38 serves as a loading control. (b) Quantitative PCR analysis of *Il12a*, *Il12b* and *Nos2* mRNA in wild-type and RBP-J-deficient BMDMs transduced with control virus or retrovirus expressing IRAK2, then left unstimulated or stimulated for 6 h with LPS at 48 h after transduction; results are normalized to *Gapdh* mRNA and are presented relative to those of unstimulated wild-type cells, set as 1. (c) Quantitative PCR analysis of *Irak2* mRNA in wild-type and RBP-J-deficient BMDMs stimulated for 0–60 min (horizontal axis) with LPS; results presented as in b. (d) SDS-PAGE of ³⁵S-labeled IRAK2 immunoprecipitated from wild-type and RBP-J-deficient BMDMs after metabolic labeling for 30–240 min (above lanes); immunoblot analysis of p38 in whole-cell lysates (below) serves as a loading control. (e) Quantification of IRAK2 in whole-cell lysates of wild-type and RBP-J-deficient BMDMs stimulated for 30 min with LPS, followed by treatment for 0–150 min (horizontal axis) with cycloheximide (20 μg/ml). (f) Immunoblot analysis of IRAK2 in whole-cell lysates of BMDMs obtained from NICD1^M mice and their wild-type littermates and stimulated for 0–60 min (above lanes) with LPS. Data are representative of at least three independent experiments (mean and s.d. of triplicates in b,c).

We examined the role of MAPKs in the TLR4-induced activation of MNK1 through the use of pharmacological inhibitors of the MAPK kinase MEK (U0126) and the MAPKs p38 (SB203580) and Jnk (SP600125); an inhibitor of the phosphorylation of eIF4E by MNK1 (CGP57380)³⁹ served as a positive control (Fig. 6b). Although inhibitors of single MAPKs had modest effects, a combination of the inhibitors of MEK and p38 effectively suppressed the TLR4-induced phosphorylation of MNK1 and eIF4E (Fig. 6b), which indicated that both Erk and p38 were necessary for activation of the MNK1 pathway by TLR4. RBP-J deficiency did not substantially alter the TLR4-induced activation of Jnk (Supplementary Fig. 6a), consistent with the idea that Jnk is dispensable for MNK1 activation. In contrast, phosphorylation of Erk and MEK (which activates Erk downstream of TLR signaling) was lower in RBP-J-deficient macrophages than in wild-type macrophages (Fig. 6c and Supplementary Fig. 6b). Furthermore, RBP-J deficiency led to less phosphorylation of p38 and its upstream kinases MKK3–MKK6 in response to stimulation with LPS (Fig. 6d and Supplementary Fig. 6b). These results indicated that regulation of the TLR4-induced activation of Erk and p38 was one mechanism by which RBP-J controlled activation of the MNK1–eIF4E axis. Although the dependence of Erk and p38 signaling on RBP-J was modest, the activation of MNK1 was dependent on RBP-J, consistent with published work suggesting a requirement for dual activation of MNK proteins by Erk and p38 (refs. 37–39).

RBP-J targets IRAK2 upstream of MNK1–eIF4E

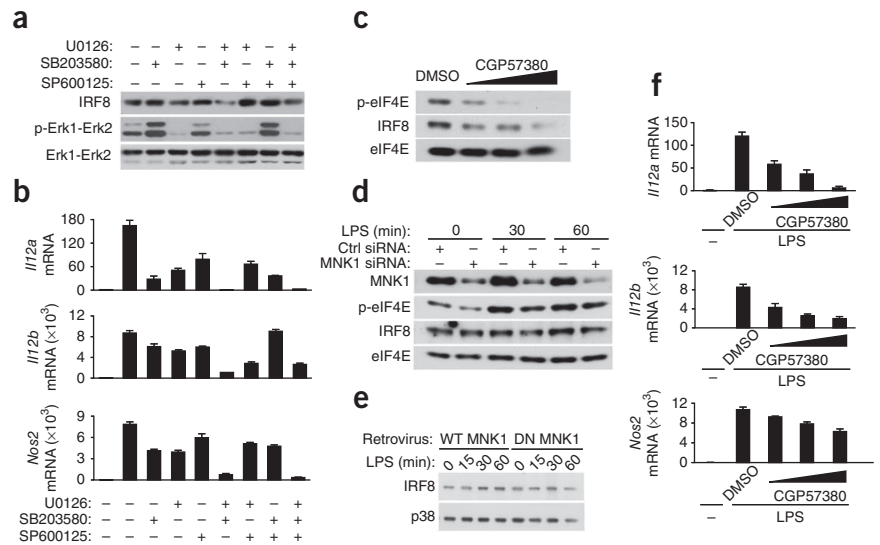
Next we investigated potential targets of RBP-J upstream of MAPKs and MNK1 in the TLR4 signaling cascades. IRAK2 is a proximal component of TLR signaling that has a role in the TLR-mediated activation of MNK1 and also functions as a post-transcriptional regulator^{38,40}. Consistent with published reports^{38,41}, acute stimulation of wild-type macrophages with LPS did not result in upregulation of IRAK2 expression (Fig. 7a). However, the expression of IRAK2 protein was much lower in RBP-J-deficient macrophages than in wild-type cells (Fig. 7a). This effect was specific, as the expression of other proteins of the IRAK family, such as IRAK1, was not lower in RBP-J-deficient macrophages than in wild-type cells (Supplementary Fig. 6c and data not shown). To determine whether diminished IRAK2 expression

contributed to the lower expression of M1 macrophage-associated genes in RBP-J-deficient cells, we restored IRAK2 expression in RBP-J-deficient macrophages by retroviral transduction. Reconstitution of IRAK2 partially corrected the phenotype (Fig. 7b), which suggested that the requirement for RBP-J in the induction of M1 macrophage-associated genes was due at least in part to the regulation of IRAK2 by RBP-J.

Next we investigated the mechanisms by which RBP-J signaling regulated IRAK2 expression. Wild-type and RBP-J-deficient cells did not have substantially different amounts of *Irak2* mRNA at baseline or after LPS stimulation (Fig. 7c), which indicated that RBP-J did not regulate *Irak2* expression. We also determined if RBP-J deficiency resulted in less synthesis of and/or more degradation of IRAK2 protein. We assessed the former by metabolic labeling assays and found that RBP-J deficiency resulted in attenuated synthesis of IRAK2 protein, as shown by less incorporation of ³⁵S-labeled methionine–cysteine at multiple labeling time points (Fig. 7d). In addition, in the presence of the protein-synthesis inhibitor cycloheximide, IRAK2 degraded at a faster rate in RBP-J-deficient macrophages than in wild-type cells under LPS-stimulated conditions (Fig. 7e). Therefore, both less synthesis and more degradation contributed to the lower abundance of IRAK2 in RBP-J-deficient cells. We also found higher expression of IRAK2 protein in NICD1^M macrophages than in wild-type macrophages (Fig. 7f). That higher expression of IRAK2 protein was not due to higher expression of *Irak2* mRNA (Supplementary Fig. 6d), which supported the idea that Notch–RBP-J signaling regulated IRAK2 expression post-transcriptionally.

To assess the role of IRAK2 in mediating RBP-J-dependent, TLR4-induced signaling events, we evaluated the activation of MAPK kinases and MAPKs in cells in which IRAK2 expression was knocked down through the use of RNA-mediated interference. Lower IRAK2 expression (Supplementary Fig. 6e) resulted in impaired activation of the MEK–Erk pathway as well as the MKK3–MKK6–p38 pathway after stimulation with LPS (Supplementary Fig. 6f) but did not affect the phosphorylation of Jnk (Supplementary Fig. 6g). Overall, these results demonstrated that the Notch–RBP-J pathway controlled a TLR4-activated MAPK–MNK1–eIF4E signaling cascade by regulating the expression of IRAK2 protein.

Figure 8 The MAPK-MNK1-eIF4E axis promotes the synthesis of IRF8 and the expression of M1 macrophage-associated genes. **(a)** Immunoblot analysis of total IRF8 and phosphorylated Erk1-Erk2 in wild-type BMDMs pretreated for 30 min with dimethyl sulfoxide (–) or various combinations (above lanes) of the MAPK inhibitors U0126, SB203580 and SP600125, then stimulated for 60 min with LPS; total Erk1-Erk2 serves as a loading control. **(b)** Quantitative PCR analysis of *Il12a*, *Il12b* and *Nos2* mRNA in wild-type BMDMs pretreated with MAPK inhibitors as in **a** and stimulated for 3 h with LPS; results are normalized to those of unstimulated cells, set as 1. **(c)** Immunoblot analysis of phosphorylated eIF4E and total IRF8 in wild-type BMDMs pretreated with for 30 min with dimethyl sulfoxide (DMSO) or increasing doses (wedge) of the MNK inhibitor CGP57380, then stimulated for 60 min with LPS; total eIF4E serves as a loading control. **(d)** Immunoblot of total MNK1, phosphorylated eIF4E and total IRF8 in wild-type BMDMs transfected with nontargeting control or MNK1-specific small interfering RNA (siRNA) and treated for 0, 30 or 60 min (top) with LPS at 2 d after transfection. **(e)** Immunoblot analysis of IRF8 in wild-type BMDMs transduced with retrovirus encoding wild-type MNK1 (WT MNK1) or a dominant-negative MNK1 mutant (DN MNK1) and stimulated for 0–60 min (above lanes) with LPS after selection for 4 d in puromycin-containing medium. **(f)** Quantitative PCR analysis of *Il12a*, *Il12b* and *Nos2* mRNA in wild-type BMDMs without pretreatment or stimulation (far left) or pretreated for 30 min with dimethyl sulfoxide or increasing doses of CGP57380, then stimulated for 3 h with LPS; results presented as in **b**. Data are representative of at least three independent experiments (**a–d,f**) or two independent experiments (**e**; error bars (**b,f**), s.d.).



MNK1-eIF4E controls the TLR4-induced synthesis of IRF8 protein

We sought to link the RBP-J-mediated regulation of MAPK-MNK1-eIF4E signaling to the regulation of the induction of IRF8 protein. In LPS-activated macrophages, IRF8 expression was much lower after the activation of both Erk and p38 was inhibited pharmacologically through the use of U0126 and SB203580, respectively, whereas the inhibition of Jnk with SP600125 did not have a discernible effect on the amount of IRF8 protein (**Fig. 8a**). The combined inhibition of Erk and p38 almost completely abolished the induction of M1 macrophage-associated genes (**Fig. 8b**) and IL-12 protein (**Supplementary Fig. 7a**) by LPS, which suggested that both Erk and p38 were necessary for the expression of IRF8 protein and the subsequent induction of M1 macrophage-associated genes in TLR4-stimulated macrophages. Treatment of macrophages with the MNK1 inhibitor CGP57380 suppressed the LPS-induced phosphorylation of eIF4E and expression of IRF8 protein in a dose-dependent manner (**Fig. 8c**). Knockdown of MNK1 in macrophages by RNA-mediated interference led to less phosphorylation of eIF4E and attenuated induction of IRF8 by LPS (**Fig. 8d** and **Supplementary Fig. 7b**). However, it did not affect the expression of *Irf8* mRNA (**Supplementary Fig. 7c**). Transduction of macrophages with a retrovirus expressing a dominant-negative mutant of MNK1 that lacks kinase activity and thus is unable to phosphorylate eIF4E⁴² blunted the LPS-activated induction of IRF8 protein (**Fig. 8e**). The inhibition of MNK1 activity by CGP57380 suppressed the TLR4-induced expression of *Il12a*, *Il12b* and *Nos2* (**Fig. 8f**) without apparent toxicity (data not shown) or global interference with TLR responsiveness (**Supplementary Fig. 7d**). Together these experiments supported the proposal of a role for MNK1-eIF4E in the TLR4-induced expression of IRF8 protein and induction of genes that are targets of IRF8. We propose a model for the regulation of the polarization of M1 macrophages through crosstalk between the Notch-RBP-J and TLR signaling pathways (**Supplementary Fig. 8**).

DISCUSSION

The selective transcription of functionally related subsets of genes in response to inflammatory stimuli is important for achieving appropriate immune responses¹¹. Here we have shown that the Notch-RBP-J pathway selectively regulated a subset of TLR4-inducible, classic M1 macrophage-associated genes, including *Il12a*, *Il12b* and *Nos2*. Signaling via RBP-J and TLR4 converged to synergistically induce rapid expression of IRF8 protein, which in turn directly activated the downstream expression of M1 macrophage-associated genes. Notch1-RBP-J signaling was required for the activity of MNK1 and eIF4E, which augmented the translation of IRF8. Our findings have provided a functional connection between Notch-RBP-J signaling and the IRF family of transcription factors and have identified a mechanism by which RBP-J and TLR4 signaling are integrated to induce the translation of a key transcription factor important to the activation of macrophages.

IRF8 expression is known to be transcriptionally inducible by IFN- γ (refs. 34,35). Here we found that LPS alone (without IFN- γ) induced rapid expression of IRF8 protein independently of the upregulation of *Irf8* mRNA; this activated a subset of TLR-inducible promoters, such as *Il12b*, in an RBP-J-dependent manner. The observations that the activation of MNK1 and subsequent phosphorylation of eIF4E are induced by inflammatory stimuli, including TLR ligands and interferons^{38,39}, suggest that this pathway may be important in promoting the translation of a select subset of transcripts under inflammatory conditions. Furthermore, Notch-RBP-J signaling controlled the amount of IRAK2 protein independently of the regulation of mRNA expression. Although IRAK2 is an integral component of the TLR signaling cascade and the amount of IRAK2 is critical for determining TLR responsiveness⁴³, little is known about how the synthesis or degradation of IRAK2 protein is regulated. The exact mechanisms by which Notch signaling regulates the expression of IRAK2 remain to be determined.

Notably, the RBP-J-dependent M1 macrophage-associated genes identified here are all secondary-response genes whose expression

is dependent on new protein synthesis. The identity of the factors responsible for the induction of secondary-response genes has remained elusive¹¹. Our results indicate that IRF8 represents such a factor. However, we were unable to rule out the possibility that RBP-J regulated the expression of TLR-inducible genes by additional mechanisms. Regulation of NF- κ B activity by RBP-J has been described⁴⁴. Because *Il12a*, *Il12b* and *Nos2* are known targets of c-Rel, we determined whether NF- κ B had a role in the RBP-J-mediated regulation of these genes. However, the acute activation of canonical NF- κ B signaling, as measured by degradation of the NF- κ B inhibitor I κ B α and nuclear accumulation of c-Rel, was not affected by RBP-J deficiency, and the expression of many canonical NF- κ B target genes was intact in RBP-J-deficient cells (data not shown), which suggested that NF- κ B was not the central point of signaling integration between the RBP-J and TLR pathways in our system. Indeed, the regulation of NF- κ B by RBP-J would be expected to have broader effects on the expression of TLR-inducible genes and could not explain the selective regulation that we observed. However, it is plausible that NF- κ B may be subject to regulation by RBP-J under other conditions, such as late-phase TLR responses in which IRAK2 contributes to sustained activation of NF- κ B (ref. 41), or in other cell types, such as T cells and human peripheral blood mononuclear cells^{40,45}.

Notch receptors and their ligands have been linked to regulating the production of inflammatory cytokines^{18,20,24}, mostly through a positive feed-forward loop in which inflammatory stimuli such as TLR ligands induce the expression of Notch receptors and/or their ligands and activate canonical Notch signaling, which in turn augments TLR-induced cytokine production in a nonselective manner. In contrast, we have shown here that the induction of IRF8 by RBP-J and TLR signaling occurred minutes after TLR stimulation, before the reported induction of the expression of Notch receptors or their ligands^{18,20,24}. Furthermore, in primary macrophages, despite the finding that Notch signaling was constitutively active at baseline, it was not further activated by TLR stimulation within the experimental time frame (X.H., data not shown), which indicated a lack of acute activation of canonical Notch signaling by TLR pathways. Thus, our data suggest a model in which constitutive Notch signaling via RBP-J serves as a 'tonic' signal that is necessary but not sufficient for gene induction and that the TLR pathway provides a 'triggering' signal that activates gene expression. Such a tonic signal would be delivered *in vivo* under baseline conditions in which Notch ligands are expressed, such as in the marginal zone of the spleen¹⁶ and in the blood circulation²⁴. Feed-forward regulation involving the induction of Notch components would then serve as an amplification loop that is potentially important for sustaining TLR responses at later time points. Overall, our findings have highlighted the selective regulation of TLR-inducible gene expression by Notch signaling that modulates inflammatory macrophage phenotype.

METHODS

Methods and any associated references are available in the online version of the paper.

Note: Supplementary information is available in the online version of the paper.

ACKNOWLEDGMENTS

We thank T. Honjo (Kyoto University) for *Rbpj*^{fllox/fllox} mice; T. Gridley (Maine Medical Center Research Institute) for *Notch1*^{+/-} mice; R. Kopan (Washington University) for NICD1 expression plasmids; S. Smale (University of California, Los Angeles) for *Il12b* promoter reporter constructs; M. Takami (Showa University) for the IRF8 expression construct; S. Akira (Osaka University) for IRAK2 retroviral constructs; J.A. Cooper (Fred Hutchinson Cancer Research Center) for MNK1 expression plasmids; E. Kieff (Harvard Medical School);

J.C. Aster (Harvard Medical School) for anti-RBP-J rabbit serum; E.G. Pamer for discussions about the *L. monocytogenes* infection experiments; and K. Au for technical assistance. Supported by the American College of Rheumatology (X.H.) and the US National Institutes of Health (L.B.I. and X.H.).

AUTHOR CONTRIBUTIONS

H.X., J.Z., J.F., A.Y.C. and C.S. did experiments and analyzed data; S.S. did experiments, analyzed data and prepared the manuscript. B.Z. generated NICD1^M mice, provided the IRF8-expressing retroviral vector and assisted with the experiments with *Irf8*^{-/-} mice; H.O. and J.K. provided *Notch1*^{+/-} mice; S.W. and P.S. provided ADAM10-deficient mice; Y.L. provided GSI34; K.O. provided *Irf8*^{-/-} mice; C.P.B. provided mice with *loxP*-flanked *Adam17* alleles and advice about experiments; L.B.I. provided advice about experiments and contributed to manuscript preparation; and X.H. designed research, supervised experiments and prepared the manuscript.

COMPETING FINANCIAL INTERESTS

The authors declare no competing financial interests.

Published online at <http://www.nature.com/doi/10.1038/ni.2304>.

Reprints and permissions information is available online at <http://www.nature.com/reprints/index.html>.

- Mosser, D.M. & Edwards, J.P. Exploring the full spectrum of macrophage activation. *Nat. Rev. Immunol.* **8**, 958–969 (2008).
- Krausgruber, T. *et al.* IRF5 promotes inflammatory macrophage polarization and T_H1–T_H17 responses. *Nat. Immunol.* **12**, 231–238 (2011).
- Satoh, T. *et al.* The Jmjd3-Irf4 axis regulates M2 macrophage polarization and host responses against helminth infection. *Nat. Immunol.* **11**, 936–944 (2010).
- Taylor, P. *et al.* The feedback phase of type I interferon induction in dendritic cells requires interferon regulatory factor 8. *Immunity* **27**, 228–239 (2007).
- Holtzman, T. *et al.* Immunodeficiency and chronic myelogenous leukemia-like syndrome in mice with a targeted mutation of the ICSBP gene. *Cell* **87**, 307–317 (1996).
- Liu, J., Guan, X., Tamura, T., Ozato, K. & Ma, X. Synergistic activation of interleukin-12 p35 gene transcription by interferon regulatory factor-1 and interferon consensus sequence-binding protein. *J. Biol. Chem.* **279**, 55609–55617 (2004).
- Xiong, H. *et al.* Complex formation of the interferon (IFN) consensus sequence-binding protein with IRF-1 is essential for murine macrophage IFN- γ -induced iNOS gene expression. *J. Biol. Chem.* **278**, 22712–22717 (2003).
- Giese, N.A. *et al.* Interferon (IFN) consensus sequence-binding protein, a transcription factor of the IFN regulatory factor family, regulates immune responses *in vivo* through control of interleukin 12 expression. *J. Exp. Med.* **186**, 1535–1546 (1997).
- Wang, H. & Morse, H.C. III. IRF8 regulates myeloid and B lymphoid lineage diversification. *Immunol. Res.* **43**, 109–117 (2009).
- Tamura, T. & Ozato, K. ICSBP/IRF-8: its regulatory roles in the development of myeloid cells. *J. Interferon Cytokine Res.* **22**, 145–152 (2002).
- Smale, S.T. Selective transcription in response to an inflammatory stimulus. *Cell* **140**, 833–844 (2010).
- Anderson, P. Post-transcriptional regulons coordinate the initiation and resolution of inflammation. *Nat. Rev. Immunol.* **10**, 24–35 (2010).
- Mazumder, B., Li, X. & Barik, S. Translation control: a multifaceted regulator of inflammatory response. *J. Immunol.* **184**, 3311–3319 (2010).
- Kopan, R. & Ilagan, M.X. The canonical Notch signaling pathway: unfolding the activation mechanism. *Cell* **137**, 216–233 (2009).
- Yuan, J.S., Kousis, P.C., Suliman, S., Visan, I. & Guidos, C.J. Functions of notch signaling in the immune system: consensus and controversies. *Annu. Rev. Immunol.* **28**, 343–365 (2010).
- Caton, M.L., Smith-Raska, M.R. & Reizis, B. Notch-RBP-J signaling controls the homeostasis of CD8⁻ dendritic cells in the spleen. *J. Exp. Med.* **204**, 1653–1664 (2007).
- Hu, X. *et al.* Integrated regulation of Toll-like receptor responses by Notch and interferon-gamma pathways. *Immunity* **29**, 691–703 (2008).
- Monsalve, E. *et al.* Notch-1 up-regulation and signaling following macrophage activation modulates gene expression patterns known to affect antigen-presenting capacity and cytotoxic activity. *J. Immunol.* **176**, 5362–5373 (2006).
- Zhou, J., Cheng, P., Youn, J.I., Cotter, M.J. & Gaboritov, D.I. Notch and wingless signaling cooperate in regulation of dendritic cell differentiation. *Immunity* **30**, 845–859 (2009).
- Foldi, J. *et al.* Autoamplification of Notch signaling in macrophages by TLR-induced and RBP-J-dependent induction of Jagged1. *J. Immunol.* **185**, 5023–5031 (2010).
- Wang, Y.C. *et al.* Notch signaling determines the M1 versus M2 polarization of macrophages in antitumor immune responses. *Cancer Res.* **70**, 4840–4849 (2010).
- Klinakis, A. *et al.* A novel tumour-suppressor function for the Notch pathway in myeloid leukaemia. *Nature* **473**, 230–233 (2011).
- Zhao, B., Grimes, S.N., Li, S., Hu, X. & Ivashkiv, L.B. TNF-induced osteoclastogenesis and inflammatory bone resorption are inhibited by transcription factor RBP-J. *J. Exp. Med.* **209**, 319–334 (2012).

24. Outtz, H.H., Wu, J.K., Wang, X. & Kitajewski, J. Notch1 deficiency results in decreased inflammation during wound healing and regulates vascular endothelial growth factor receptor-1 and inflammatory cytokine expression in macrophages. *J. Immunol.* **185**, 4363–4373 (2010).
25. Serbina, N.V., Jia, T., Hohl, T.M. & Pamer, E.G. Monocyte-mediated defense against microbial pathogens. *Annu. Rev. Immunol.* **26**, 421–452 (2008).
26. Swiatek, P.J., Lindsell, C.E., del Amo, F.F., Weinmaster, G. & Gridley, T. Notch1 is essential for postimplantation development in mice. *Genes Dev.* **8**, 707–719 (1994).
27. Murtaugh, L.C., Stanger, B.Z., Kwan, K.M. & Melton, D.A. Notch signaling controls multiple steps of pancreatic differentiation. *Proc. Natl. Acad. Sci. USA* **100**, 14920–14925 (2003).
28. Plevy, S.E., Gemberling, J.H., Hsu, S., Dorner, A.J. & Smale, S.T. Multiple control elements mediate activation of the murine and human interleukin 12 p40 promoters: evidence of functional synergy between C/EBP and Rel proteins. *Mol. Cell Biol.* **17**, 4572–4588 (1997).
29. Grumont, R. *et al.* c-Rel regulates interleukin 12 p70 expression in CD8⁺ dendritic cells by specifically inducing p35 gene transcription. *J. Exp. Med.* **194**, 1021–1032 (2001).
30. Xie, Q.W., Kashiwabara, Y. & Nathan, C. Role of transcription factor NF- κ B/Rel in induction of nitric oxide synthase. *J. Biol. Chem.* **269**, 4705–4708 (1994).
31. Masumi, A., Tamaoki, S., Wang, I.M., Ozato, K. & Komuro, K. IRF-8/ICSBP and IRF-1 cooperatively stimulate mouse IL-12 promoter activity in macrophages. *FEBS Lett.* **531**, 348–353 (2002).
32. Ramirez-Carrozzi, V.R. *et al.* Selective and antagonistic functions of SWI/SNF and Mi-2beta nucleosome remodeling complexes during an inflammatory response. *Genes Dev.* **20**, 282–296 (2006).
33. Zhang, J. *et al.* Activation of IL-27 p28 gene transcription by interferon regulatory factor 8 in cooperation with interferon regulatory factor 1. *J. Biol. Chem.* **285**, 21269–21281 (2010).
34. Kantakamalaku, W. *et al.* Regulation of IFN consensus sequence binding protein expression in murine macrophages. *J. Immunol.* **162**, 7417–7425 (1999).
35. Zhao, J. *et al.* IRF-8/interferon (IFN) consensus sequence-binding protein is involved in Toll-like receptor (TLR) signaling and contributes to the cross-talk between TLR and IFN- γ signaling pathways. *J. Biol. Chem.* **281**, 10073–10080 (2006).
36. Xiong, H. *et al.* Ubiquitin-dependent degradation of interferon regulatory factor-8 mediated by Cbl down-regulates interleukin-12 expression. *J. Biol. Chem.* **280**, 23531–23539 (2005).
37. Ueda, T., Watanabe-Fukunaga, R., Fukuyama, H., Nagata, S. & Fukunaga, R. Mnk2 and Mnk1 are essential for constitutive and inducible phosphorylation of eukaryotic initiation factor 4E but not for cell growth or development. *Mol. Cell Biol.* **24**, 6539–6549 (2004).
38. Wan, Y. *et al.* Interleukin-1 receptor-associated kinase 2 is critical for lipopolysaccharide-mediated post-transcriptional control. *J. Biol. Chem.* **284**, 10367–10375 (2009).
39. Joshi, S. *et al.* Essential role for Mnk kinases in type II interferon (IFN γ) signaling and its suppressive effects on normal hematopoiesis. *J. Biol. Chem.* **286**, 6017–6026 (2011).
40. Flannery, S.M., Keating, S.E., Szymak, J. & Bowie, A.G. Human interleukin-1 receptor-associated kinase-2 is essential for Toll-like receptor-mediated transcriptional and post-transcriptional regulation of tumor necrosis factor α . *J. Biol. Chem.* **286**, 23688–23697 (2011).
41. Kawagoe, T. *et al.* Sequential control of Toll-like receptor-dependent responses by IRAK1 and IRAK2. *Nat. Immunol.* **9**, 684–691 (2008).
42. Waskiewicz, A.J., Flynn, A., Proud, C.G. & Cooper, J.A. Mitogen-activated protein kinases activate the serine/threonine kinases Mnk1 and Mnk2. *EMBO J.* **16**, 1909–1920 (1997).
43. Conner, J.R., Smirnova, I. & Poltorak, A. A mutation in *Irak2c* identifies IRAK-2 as a central component of the TLR regulatory network of wild-derived mice. *J. Exp. Med.* **206**, 1615–1631 (2009).
44. Osipo, C., Golde, T.E., Osborne, B.A. & Miele, L.A. Off the beaten pathway: the complex cross talk between Notch and NF- κ B. *Lab. Invest.* **88**, 11–17 (2008).
45. Shin, H.M. *et al.* Notch1 augments NF- κ B activity by facilitating its nuclear retention. *EMBO J.* **25**, 129–138 (2006).

ONLINE METHODS

Cells and reagents. Mouse BMDMs were obtained as described¹⁷ and were maintained in DMEM supplemented with 10% FBS and 10% supernatants of L929 mouse fibroblasts as conditioned medium providing macrophage colony-stimulating factor (M-CSF). Recombinant mouse IFN- γ was from Peprotech and was used at concentration of 10 ng/ml. Cell-culture-grade LPS and cycloheximide were from Sigma-Aldrich. Pam₃Cys was from EMC Microcollections. LPS was used at concentration of 1 ng/ml and Pam₃Cys was used at concentration of 10 ng/ml unless otherwise noted. The γ -secretase inhibitor GSI34 was used at concentration of 10 μ M as described⁴⁶. U0126, SB203580, SP600125 and CGP57380 were from Calbiochem.

Mice. Experiments with mice were approved by Institutional Animal Care and Use Committees at the Hospital for Special Surgery, Columbia University, and Christian Albrechts Universität Kiel. C57/BL6 mice were from Jackson Laboratory. *Rbpj*^{fllox/fllox} mice were provided by T. Honjo. Mice with myeloid cell-specific deletion of *Rbpj* (*Rbpj*^{fllox/fllox}*Lyz2-Cre*) have been described¹⁷ and were used for *in vivo* experiments, given the tissue specificity of the deletion. Mice with inducible deletion of *Rbpj* (*Rbpj*^{fllox/fllox}*Mx1-Cre*) were generated by crossing of *Rbpj*^{fllox/fllox} mice to mice expressing a *Mx1* promoter-driven transgene encoding Cre, on the C57/BL6 background (Jackson Laboratory). Littermates with an *Rbpj*^{fllox/fllox}*Mx1-Cre* or *Rbpj*^{+/+}*Mx1-Cre* genotype were given intraperitoneal injection of poly(I:C) at a dose of 200 μ g per mouse three times in 5 d to induce deletion and mice were used for experiments 2 weeks later. For all *in vitro* experiments involving RBP-J-deficient macrophages, cells were derived from *Rbpj*^{fllox/fllox}*Mx1-Cre* mice where substantial deletion of *Rbpj* (approximately 80%) was observed; the conditional deletion was controlled for expression of Cre and genetic background through the use of cells from *Rbpj*^{+/+}*Mx1-Cre* mice. *Adam10*^{fllox/fllox} mice have been described⁴⁷, and *Adam10*^{fllox/fllox}*Mx1-Cre* mice were generated and used by a procedure similar to that described for *Rbpj*^{fllox/fllox}*Mx1-Cre* mice. *Adam17*^{fllox/fllox}*Lyz2-Cre* mice were generated by crossing of *Adam17*^{fllox/fllox} mice⁴⁸ to *Lyz2-Cre* mice on the C57/BL6 background (Jackson Laboratory). *Notch1*^{+/-} mice were provided by T. Gridley²⁶. *Rosa*^{Notch} mice, in which cDNA encoding constitutively active mouse NICD1 was knocked into the ubiquitously expressed *Rosa26* locus, followed by sequence encoding an internal ribosome entry site and enhanced green fluorescent protein (eGFP), and preceded by a fragment encoding a stop signal, flanked by *loxP* sites²⁷, were from the Jackson Laboratory. Mice with myeloid cell-specific constitutive expression of NICD1 (*NICD1*^M mice) were generated by the crossing of *Rosa*^{Notch} mice with *Lyz2-Cre* mice. Sex- and age-matched *Lyz2-Cre* mice were used as controls. *NICD1*^M macrophages were obtained by culture of bone marrow cells from *NICD1*^M mice for 5 d in conditioned medium containing M-CSF. At the end of the culture period, adherent cells were collected and replated for experiments. *Irf8*^{-/-} mice have been described⁵. All experiments involving knockout mice used sex-matched littermates of the desired genotype as a control. Bone marrow chimeras were generated as described⁴⁹. Recipient C57BL/6 mice were subjected to irradiation at a dose of 1,000 cGy, followed by intravenous injection of 1×10^6 donor bone marrow cells from mice with myeloid cell-specific RBP-J deficiency (*Rbpj*^{fllox/fllox}*Lyz2-Cre*) or their wild-type (*Rbpj*^{+/+}*Lyz2-Cre*) littermates as controls. Chimeric mice were used for experiments 6 weeks after the initial bone marrow transfer.

Isolation of mRNA and quantitative PCR. RNA was extracted from whole-cell lysates with an RNeasy Mini kit (Qiagen) and was reverse-transcribed with a First Strand cDNA synthesis kit (Fermentas). Quantitative PCR was done in triplicate wells with an iCycler IQ thermal cycler and detection system (Bio-Rad) with gene-specific primers. Threshold cycle numbers were normalized to those of triplicate samples amplified with primers specific for glyceraldehyde-3-phosphate dehydrogenase (*Gapdh*).

Enzyme-linked immunosorbent assay. Cytokine secretion was quantified with ELISA kits from BD Pharmingen, and the production of nitric oxide was measured with Greiss reagent according to manufacturers' instructions (Sigma).

L. monocytogenes infection. Mice were infected intravenously with 3×10^3 *L. monocytogenes* strain 10403S, as described⁴⁹. At day 3.5 after infection,

spleens and livers were collected and dissociated in PBS containing 0.05% Triton X-100, and bacterial colony-forming units were determined by plating on brain-heart-infusion agar plates.

Immunoblot analysis. Whole-cell lysates were prepared by direct lysis in SDS loading buffer. For immunoblot analysis, lysates were separated by 10% SDS-PAGE and transferred to a polyvinylidene difluoride membrane for probing with antibody. Polyclonal antibody to IRF8 (anti-IRF8; C-19), anti-p38 (C-20), anti-c-Rel (C), anti-TBP (SI-1) and anti-SHP2 (D-17) were from Santa Cruz Biotechnology. Anti-IRAK2 (ab62419) and anti- β -tubulin (ab6046) were from Abcam. Antibody to MEK1-MEK2 phosphorylated at Ser217 and Ser221 (9154), MKK3-MKK6 phosphorylated at Ser189 and Ser207 (9231), Jnk phosphorylated Thr183 and Tyr185 (9251), Erk phosphorylated Thr202 and Tyr204 (9101), p38 phosphorylated Thr180 and Tyr182 (9215), MNK1 phosphorylated Thr197 and Thr202 (2111), eIF4E phosphorylated Ser209 (9741), and anti-MNK1 (2195), anti-eIF4E (2067), anti-Ik β (4812), anti-IRF4 (4948), anti-IRF5 (4950) and anti-Erk1-Erk2 (9102) were from Cell Signaling. Anti-RBP-J rabbit serum was a gift from E. Kieff and J.C. Aster⁵⁰.

Transient transfection and luciferase assay. A luciferase reporter plasmid containing sequences from positions -356 to +55 of the mouse *Il12b* promoter was provided by S.T. Smale. RAW264.7 cells were transfected in duplicate with the *Il12b* reporter plasmid and an expression vector encoding NICD1 (a gift from R. Kopan) through the use of Lipofectamine LTX reagent (Invitrogen). The pRL-TK plasmid encoding renilla luciferase (Promega) was used as an internal control. A Dual-Luciferase Reporter Assay System (Promega) was used for the detection of luciferase activity of cell lysates 36 h after transfection.

RNA-mediated interference. Small interfering RNA (siRNA) specifically targeting mouse Notch2, IRAK2 or MNK1, and nontargeting control siRNA were from Dharmacon. The siRNA was transfected into mouse BMDMs through the use of TransIT TKO transfection reagent according to the manufacturer's instructions (Mirus Bio).

Chromatin immunoprecipitation. This assay was done as described¹⁷ with slight modifications. Cells (8×10^6 to 10×10^6) were crosslinked with 0.75% formaldehyde. After being lysed in 8 ml lysis buffer, the pellets were resuspended in cold radioimmunoprecipitation buffer and were sonicated on ice at power setting 5 in 20-second bursts for six cycles. Lysates were then cleared by centrifugation and were incubated overnight with rotation with 2 μ g goat anti-IRF8 (C-19; Santa Cruz Biotechnology) or monoclonal antibody to RNA polymerase II (05-623; Millipore). The same amount of normal goat IgG (sc2028; Santa Cruz Biotechnology) or normal mouse IgG (MABC002; Millipore), respectively, was used as a control. Antibody incubation was followed by incubation for 1.5 h at 4 $^{\circ}$ C with 45 μ l of 33% Protein A/G agarose slurry (Santa Cruz Biotechnology). Then, the agarose slurry bond complexes were digested with proteinase K and phenol-chloroform was used to purify DNA for quantitative PCR. Unrelated 28S rRNA was used for normalization of the results of quantitative PCR. The value obtained with IgG in untreated cells (control) was set as 1. Primers used for quantitative PCR were as follows: *Il12b* locus forward, 5'-CACACTGGACCAAAGGGACT-3', and reverse, 5'-CTTTGCTTCCCTAGCACCT-3'; 28S rRNA forward, 5'-GATCCTTCGATGTCGGCTCTTCCATC-3', and reverse, 5'-AGGGTAAAACTAACCTGTCTCACG-3'.

Metabolic labeling. BMDMs (8×10^6 to 10×10^6) cultured in complete medium were starved for 30 min in methionine- and cysteine-free DMEM supplemented with 5% dialyzed FBS. Then, the cells were labeled with ³⁵S-Methionine/cysteine Labeling Mix (PerkinElmer) at a final concentration of 100 μ Ci/ml. At the end of the labeling period, cells were washed twice with cold PBS and were lysed in 500 μ l lysis buffer (50 mM Tris-HCl, pH 8.0, 150 mM NaCl, 10% glycerol, 1 mM EGTA, 0.2 mM EDTA, 1% Nonidet P-40 and 1 mM dithiothreitol) supplemented with protease inhibitors (Roche). Goat polyclonal anti-IRF8 (C-19; Santa Cruz Biotechnology) and rabbit polyclonal anti-IRAK2 (ab62419; Abcam) were used for immunoprecipitation of IRF8 and IRAK2, respectively. Immunoprecipitates were resuspended in

20 μ l SDS-PAGE loading buffer for subsequent electrophoresis through a 7.5% SDS-PAGE. Gels were dried and placed on film for autoradiography overnight at -80°C .

Retroviral transduction. Plat-E cells seeded at a density of 2×10^6 per well into six-well plates were cultured overnight and then transfected with Fugene HD (Roche) and 3 μ g retroviral vector. After 48 h, viral supernatants were collected and centrifuged (1,500 r.p.m.). Viral supernatants (1.5 ml) were used for the transduction of 4×10^5 BMDMs in the presence of 8 μ g/ml polybrene (Sigma). BMDMs were used for assay 48 h after viral transduction. For transduction based on the pMx-Puro vector, virus-transduced macrophages were selected for 4 d in puromycin-containing medium before being replated for assays. The pMX-*Irf8*-IRES-EGFP retroviral vector and pMX-IRES-EGFP control vector were provided by M. Takami. A retroviral construct encoding IRAK2 and an empty-vector control construct were gifts from S. Akira⁴¹. Expression constructs for wild-type and dominant-negative (T197A,T202A) MNK1 were provided by J.A. Cooper⁴², and cDNA fragments encoding wild-type and dominant-negative MNK1 were subcloned into the pMx-Puro retroviral vector.

Flow cytometry. BMDMs were collected after 5 d of culture in conditioned medium containing M-CSF and were stained with allophycocyanin-conjugated anti-CD11b (553312; BD Pharmingen) and phycoerythrin-conjugated anti-F4/80 (MF48004; Invitrogen). Cells were washed three times and analyzed on a FACScan flow cytometer (BD) with CellQuest software (BD).

46. Shelton, C.C., Tian, Y., Frattini, M.G. & Li, Y.M. An exo-cell assay for examining real-time γ -secretase activity and inhibition. *Mol. Neurodegener.* **4**, 22 (2009).
47. Jorissen, E. *et al.* The disintegrin/metalloproteinase ADAM10 is essential for the establishment of the brain cortex. *J. Neurosci.* **30**, 4833–4844 (2010).
48. Horiuchi, K. *et al.* Cutting edge: TNF- α -converting enzyme (TACE/ADAM17) inactivation in mouse myeloid cells prevents lethality from endotoxin shock. *J. Immunol.* **179**, 2686–2689 (2007).
49. Shi, C. *et al.* Bone marrow mesenchymal stem and progenitor cells induce monocyte emigration in response to circulating toll-like receptor ligands. *Immunity* **34**, 590–601 (2011).
50. Wang, H. *et al.* Genome-wide analysis reveals conserved and divergent features of Notch1/RBPJ binding in human and murine T-lymphoblastic leukemia cells. *Proc. Natl. Acad. Sci. USA* **108**, 14908–14913 (2011).